# Supplementary Material: Deformation and Clustering of Red Blood Cells in Microcapillary Flows

J. Liam McWhirter,[1,*] Hiroshi Noguchi,[1,2,†] and Gerhard Gompper[1,‡]

[1] *Theoretical Soft Matter and Biophysics, Institute of Complex Systems, Forschungszentrum Jülich, 52425 Jülich, Germany*

[2] *Institute for Solid State Physics, University of Tokyo, Kashiwa, Chiba 277-8581, Japan*

In this supplement, we provide additional material which illustrates the shape changes of a regular array of RBCs at high tube hematocrit $H_T$, and further describes the cell clustering of an irregular RBC array at low $H_T$.

## I. MOVIE CAPTIONS

### A. Movie S1: Clustering of Six Cells in Fast Flow

The movie shows the clustering behavior of six cells in a capillary in fast flow (with $g^* = 20.4$). Starting from an aligned configuration of discocytes with no flow, the cells form of stable six-cell cluster. The parameters are $L_Z/R_0 = 14$ and $R_{\rm cap}/R_0 = 1.4$, corresponding to a hematocrit of $H_{\rm T} = 0.084$.

### B. Movie S2: Clustering of Six Cells in Medium Flow

The movie shows the clustering behavior of six cells in a capillary in medium flow (with $g^* = 15.9$). At this flow rate, the formation of small clusters and the break-up of clusters is observed frequently. The parameters are $L_Z/R_0 = 14$ and $R_{\rm cap}/R_0 = 1.4$, corresponding to a hematocrit of $H_{\rm T} = 0.084$.

### C. Movie S3: Clustering of Three Cells in Fast Flow

The movie shows the clustering behavior of three cells in a capillary in fast flow (with $g^* = 20.4$). Starting from an aligned configuration of discocytes with no flow, the cells form of stable three-cell cluster. The parameters are $L_Z/R_0 = 14$ and $R_{\rm cap}/R_0 = 1.4$, corresponding to a hematocrit of $H_{\rm T} = 0.084$.

### D. Movie S4: Clustering of Three Cells in Medium Flow

The movie shows the clustering behavior of three cells in a capillary in medium flow (with $g^* = 13.2$). At this flow rate, the formation and break-up of clusters is observed frequently. The parameters are $L_Z/R_0 = 14$ and $R_{\rm cap}/R_0 = 1.4$, corresponding to a hematocrit of $H_{\rm T} = 0.084$.

### E. Movie S5: Clustering of Three Cells in Slow Flow

The movie shows the clustering behavior of three cells in a capillary in medium flow (with $g^* = 5.4$). At this flow rate, the cells display a discocyte shape and show no tendency for clustering. The parameters are $L_Z/R_0 = 14$ and $R_{\rm cap}/R_0 = 1.4$, corresponding to a hematocrit of $H_{\rm T} = 0.084$.

## II. SHAPE TRANSITIONS OF A REGULAR ARRAY OF RBCS

In Sec. IIIB of the main text, we describe the shape changes of a single RBC ($n_{\rm ves} = 1$) in short tube segments with periodic boundary conditions, corresponding to an infinitely long capillary with a file of RBCs at fixed distances. At $H_{\rm T} \gtrsim 0.19$ (or $L_Z/R_0 \lesssim 2$), the transition in shape from discocyte to parachute is gradual. Figure 1 shows snapshots of RBCs in this regime of high hematocrit $H_{\rm T}$, starting at low $g^*$ with a discocyte whose symmetry axis is tilted away from the capillary axis (see Fig. 1, bottom), proceeding through a shape similar to a slipper whose degree of deformation away from the discocyte increases with increasing $g^*$ (see Fig. 1, middle), and finally reaching a bowl or parachute shape at high $g^*$ (see Fig. 1, top).

## III. CLUSTERING IN DILUTE SUSPENSION: THREE CELLS IN A CAPILLARY

At flow rates larger than the critical value of the discocyte-to-parachute transition, we observe clustering of cells in a dilute suspension ($H_{\rm T} = 0.084$ and $R_{\rm cap}/R_0 = 1.4$) for a simulation box with several cells

*Electronic address: j.mcwhirter@fz-juelich.de
†noguchi@issp.u-tokyo.ac.jp
‡g.gompper@fz-juelich.de

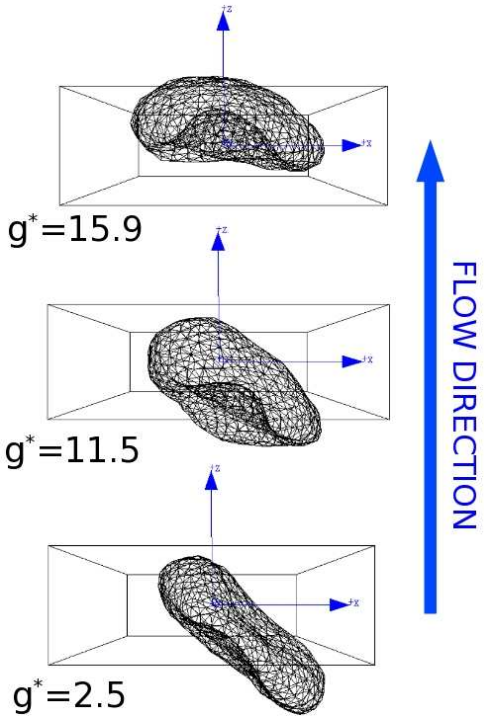


FIG. 1: Snapshots of RBCs in a concentrated suspension in a cylindrical capillary with $n_{\rm ves} = 1$, $L_Z/R_0 = 1.4$, and $R_{\rm cap}/R_0 = 1.4$ ($H_{\rm T} = 0.28$). The driving force $g^*$, and thereby the flow velocity, increases from bottom to top. The box highlights the maximum dimensions of the capillary, and should not be confused with the capillary walls.

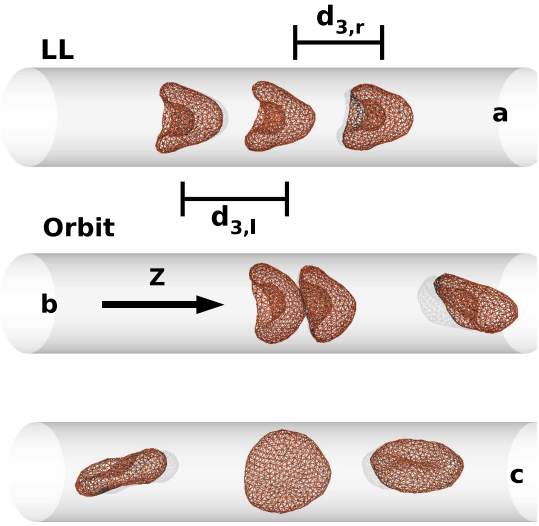


FIG. 2: Snapshots of RBCs in dilute suspension at $n_{\rm ves} = 3$, $L_Z/R_0 = 14$, and $R_{\rm cap}/R_0 = 1.4$ ($H_{\rm T} = 0.084$). (a) A loose (LL) three-cell cluster at $g^* = 20.37$ where the cells exist as parachutes (rightmost and leftmost distances are $d_{3,r}$ and $d_{3,l}$, respectively) (see Movie S3). (b) Orbiting event at $g^* = 13.15$ where the two, leftmost cells exist as shallow bowls and the third, rightmost cell as a slipper (see Movie S4). (c) Absence of clustering at $g^* = 5.37$ where the cells exist as discocytes (see Movie S5).

($n_{\rm ves} = 6$ or $n_{\rm ves} = 3$). As the flow rate or $g^*$ increases, the clusters become increasingly stable, showing no break-up and associated orbiting events.

Figure 2a,b and Movies S3, S4 show clusters in simulations with $n_{\rm ves} = 3$ cells in the simulation volume (with periodic boundary conditions in the flow direction). 3-cell clusters appear to be stable, particularly at the highest $g^*$, but infrequent "orbiting" events occur where a 3-cell cluster breaks up into a 2-cell cluster and a "free" cell, which then orbits through the periodic boundary of the capillary in a frame co-moving with the 2-cell cluster (Fig. 2). During these events, the free cell is often the shape of a slipper, and moves fastest relative to the other cells when it has this shape. With decreasing $g^*$, approaching the critical value $g_{\rm c}^*$ where an isolated cell displays a parachute-to-discocyte transition, the frequency of such "orbiting" events increased. Two 3-cell cluster states are observed: a loose (LL) state and a compact (CC) state. The LL state was the dominant state at high $g^*$. At $g^* < g_{\rm c}^*$, the cells, existing as discocytes, showed no tendency to cluster (see Movie S5). Two critical distances (center-of-mass separations of neighboring cells) mark different degrees of hydrodynamic independence and the boundaries between the CC and LL states (see Fig. 12 of main text, specifically the value of $z^*$ where the first peak in $G(z^*)$ essentially disappears with increasing $z^*$). When the center-of-mass separation between adjacent cells is less than $\Delta z_1/R_0 \sim 2$ within a 3-cell cluster, then this cluster exists in the CC state: consistent with the results described in Sec. II text (*i.e.* $L_Z/R_0 \lesssim 2$), the cell shape here is affected by neighboring cells, appearing as a shallow bowl. However, when the center-of-mass separation is greater than $\Delta z_1/R_0 \sim 2$ but less than $\Delta z_2/R_0 \sim 3$ to 3.5, then the 3-cell cluster exists in the LL state: effective hydrodynamic interactions here must be strong enough to stabilize the cluster, but not sufficiently strong to affect the cell shape, which appears as a parachute. For for a rigid, axisymmetric, periodic array, Skalak and coworkers [1, 2] found that rigid cells become hydrodynamically independent once the cells are spaced more than one capillary diameter apart; this diameter is $2R_{\rm cap}/R_0 = 2.8$ in our study.

Next, we discuss a particular dependence of the pressure drop on the cell spacing within a loose cluster. The pressure-drop (per cell) distribution, $p(\Delta P_{\rm drp})$, is shown in Fig. 3. For a loose (LL) 3-cell cluster at $g^* = 20.37$ the peak is slightly shifted to larger $\Delta P_{\rm drp}$ as $d_{3,r}$ increases from $d_{3,r}/R_0 = 2.3$ to 3, and then to 3.7; thus, the average disturbance or resistance to flow decreases as $d_{3,r}$ decreases. The response of the suspension is dominated by fluctuations; the $p(\Delta P_{\rm drp})$ widths are relatively large: $\sigma(\Delta P_{\rm drp} R_{\rm cap}^2/\eta_0 v_m R_0) \simeq 1.5$ to 2, while the shift along $\Delta P_{\rm drp} R_{\rm cap}^2/\eta_0 v_m R_0$ was about 0.2 to 0.5. Curiously, this shift is consistent with the trend in the relative apparent viscosity predicted for a model blood cell suspension of axisymmetrically-placed rigid cells as this

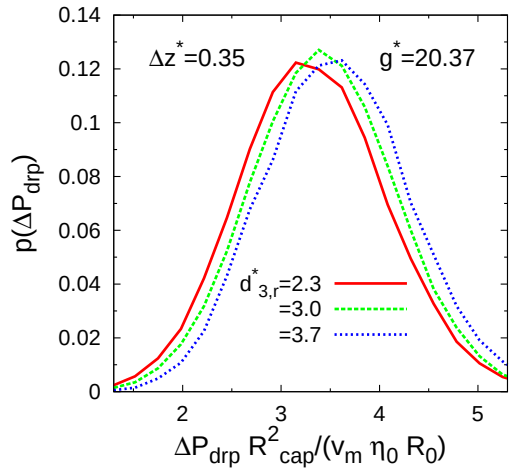


FIG. 3: Pressure drop (per cell) distributions of a loose (LL) 3-cell cluster at $g^* = 20.37$, $L_Z/R_0 = 14$, and $R_{\rm cap}/R_0 = 1.4$ for different values of the rightmost distance $d_{3,r}$ where $\Delta z^*$ is the size of the bin centered on $d_{3,r}$.

suspension goes from a 5-cell to a 3-cell rouleaux, then to a 1-cell rouleaux, at a fixed hematocrit [3]: here the viscosity was shown to increase, though only slightly at the low hematocrits. Combining our observations with these predictions, we therefore conclude that clustering slightly reduces the resistance to the fluid flow, provided there are no significant changes in the shape of the cells (for example, staying within the LL state). In our simulations, no trend in $r_{\rm max}$ was observed for variations in $d_{3,r}/R_0$ within the range $2 \lesssim d_{3,r}/R_0 \lesssim 3.7$ for the LL state. This slight decrease in pressure drop for variations in $d_{3,r}/R_0$ within the LL state should be contrasted with the relatively large increase in pressure drop we observed when going from the LL to the CC state where the cells did change shape (see Fig. 15 of main text).

Fig. 4a shows a radial distribution function $p_r(r^*_{\rm cm})$ for the center-of-mass position for the three individual cells within a 3-cell cluster in the LL state; the main text gives distributions obtained by dividing these functions by $2\pi r_{\rm cm}$ (see Fig. 16 of main text). Note that these functions are proportional to the probability of finding the center of mass of an RBC at a *radial distance* $r_{\rm cm}$ from the axis, as opposed to the probability of finding an RBC at a *given point* that is a distance $r_{\rm cm}$ away from the axis (shown in Fig. 16 of the main text).

The radial distributions of $\bar{r}_{\rm cm} = (1/3)\sum_i r_{\rm cm,i}$ for a 3-cell cluster in the LL state, where $i \in \{l, m, r\}$, are shown in Fig. 4a. With decreasing $g^*$, the distribution shifts to larger $\bar{r}_{\rm cm}$; as $g^*$ decreases, the magnitude of the lift force decreases [4, 5]. Curiously, the distribution $p_r(\bar{r}_{\rm cm})$ changes drastically in appearance between $g^* = 20.37$ and $g^* = 15.93$. This change signals the emergence of uncorrelated or unsynchronized fluctuations in the relative motions off-axis of the individual RBCs; specifically, the $r_{\rm cm}$ fluctuations of any given RBC became more uncorrelated with the $r_{\rm cm}$ fluctuations of its neighbors. In other words, at higher $g^*$ all the RBCs in a cluster moved radially off-axis more in unison than at lower $g^*$. These changes can also be observed by comparing, for example, the histograms of $\Delta r_{\rm cm} = [(1/3)\sum_{i,j}(r_{\rm cm,i} - r_{\rm cm,j})^2]^{(1/2)}$ (see Fig. 4b). As $g^*$ decreases, $p_r(\Delta r_{\rm cm})$ shifts to increasing $\Delta r_{\rm cm}$.

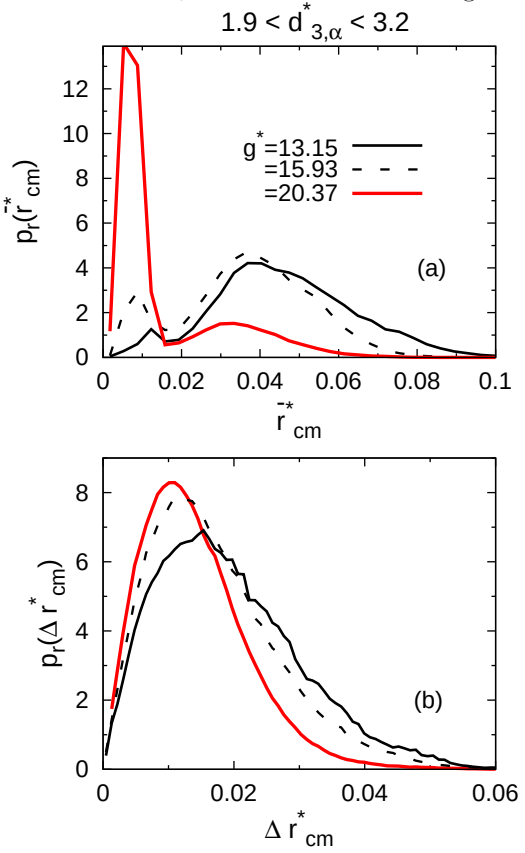


FIG. 4: (a) Radial distribution function $p_r$ of the instantaneous average of the cell center-of-mass radial positions, $r_{\rm cm}/R_0$, over the three RBCs within a 3-cell cluster in the loose (LL) internal state $[1.9 < d_{3,\alpha}/R_0 < 3.2]$ at $g^* = 20.37$, 15.93, and 13.15 for $n_{\rm ves} = 3$, $L_Z/R_0 = 14$, and $r_{\rm cap}/R_0 = 1.4$. (b) Distributions of the deviation $\Delta r_{\rm cm}$ for the LL, 3-cell cluster.

[1] H. Wang and R. Skalak, J. Fluid Mech. **38**, 75 (1969).
[2] R. Skalak, Biorheology **27**, 277 (1990).
[3] R. Skalak, P. Chen, and S. Chien, Biorheology **9**, 67 (1972).
[4] S. Sukumaran and U. Seifert, Phys. Rev. E **64**, 011916 (2001).
[5] M. Abkarian and A. Viallat, Biophys. J. **89**, 1055 (2005).